An Immune-related Signature Predicted Survival in Patients With Kidney Papillary Cell Carcinoma

Shen junwen
the first hospital of huzhou
Wang rongjiang
the first hospital of huzhou
Chen yu
the first hospital of huzhou
Fang zhihai
the first hospital of huzhou
Tang jianer
the first hospital of huzhou
Yao jianxiang
the first hospital of huzhou
Ling yuhang
the first hospital of huzhou
Zhang Lisha (zls688757@163.com)
the first hospital of huzhou
Zhang xu
Zhejiang University of Science and Technology

Research Article

Keywords: immune-related genes, Kidney papillary cell carcinoma, prognostic signature

Posted Date: March 10th, 2021

DOI: https://doi.org/10.21203/rs.3.rs-262836/v1

An immune-related signature predicted survival in patients with Kidney papillary cell carcinoma

Shen junwen[1], Wang rongjiang[1], Chen yu[1], Fang zhihai[1], Tang jianer[1], Yao jianxiang[1], Ling yuhang[1], Zhang Lisha[1] , Zhang xu[2]
1: the first hospital of Huzhou, Zhejiang province, China; 2: zhejiang university of science and technology, Zhejiang province, China
The corresponding author: Zhang Lisha, E-mail address: zls688757@163.com

Abstract: Immune-related genes are important factors in tumor progression. The main aim of this study was to identify the immune-related genes in Kidney papillary cell carcinoma (pRCC) patients. We downloaded RNAseq data and clinical information of pRCC patients from the TCGA database and retrieved the immune-related genes list from Immport. From the data, we mined out 2468 differential expression genes (DEGs) and 183 immune-related DEGs. Four hub DEGs (*NTS*, *BIRC5*, *ELN*, and *CHGA*) were identified after conducting Cox analysis and LASSO analysis. Moreover, the prognostic value of the signature based on 4 hub DEGs was verified using Kaplan-Meier analysis (P=0.0041 in the training set and p=0.021 in the test set) and ROC analysis (AUC: 0.957 in 1 year, 0.965 in 2 years, and 0.901 in 3 years in the training set, and 0.963 in 1 year, 0.898 in 2 years, and 0.742 in 3 years in the test set). Furthermore, we found that the high-risk score group had a higher percentage of B cells in the immune component, a higher expression of immune-related genes (*CTLA4*, *LAG3*, *PDCD1LG2*, and *TIGIT*), and a better immunotherapy response.

Keywords: immune-related genes, Kidney papillary cell carcinoma, prognostic signature.

Introduction

Kidney papillary cell carcinoma (pRCC) is the second most common type of renal cancer after renal clear cell carcinoma[1]. It is worth noting that the first choice treatment method for pRCC patients is maximum resection of the tumor. However, a previous study reported that partially treated patients face the challenge of disease progression[2]. Therefore, immunotherapy has become the latest choice for advanced metastatic pRCC patients[3]. Several new clinical trials have shown that immunotherapy can extend the overall survival time or delay tumor progression in partially advanced metastatic pRCC patients[4,5]. However, different trials exhibited different rates of clinical benefits. Moreover, all the trials have proven that immunotherapy is not beneficial to partially treated patients. According to EAU guidelines[6], immunotherapy was a second-line therapy option for advanced metastatic pRCC patients by the end of 2020.

The prognostic value of immune-related genes has become a subject of persistent focus in cancer research. Several previous studies have reported that some special immune-related genes or the signature had a significant survival prognostic value for tumor patients[7,8]. Our comprehensive literature review indicated that only few studies focused on the immune-related genes in pRCC patients. Therefore, we used COX analysis and LASSO analysis in this study to identify the valuable immune-related genes in pRCC patients. In addition, we developed an immune-related signature and validated its survival value.

Methods and Results

Identification of immune-related genes using differential expression data

We downloaded the gene expression RNAseq data and clinical phenotype of TCGA kidney papillary cell carcinoma (KIRP) from the UCSC Xena database (https://xenabrowser.net/datapages/). In total, we obtained 321 sample data which contained 289 cases of kidney papillary cell carcinoma (pRCC) and 32 normal samples. The data was then pre-processed with the cancer tissue using the following steps: 1. Exclusion of the samples without clinical data; 2. Exclusion of genes with FPKM <1 from all samples. Finally, we enrolled 289 pRCC and 32 normal samples. Among them, 2468 differentially expressed genes (DEGs): 638 up-regulated genes and 1830 downregulated genes (fig 1 A-B), were identified using R package "limma" (condition: adjust P.Value<0.01, and |logFC|>2)[9]. Furthermore, we downloaded the list of the immune-related genes from the ImmPort Portal database (https://www.immport.org/home/) which contained 2483 immune-related genes[10]. Intersection of the immune-related genes and 2483 DEGs resulted in the identification of 183 immune-related DEGs.

Functional and pathway enrichment analysis of immune-related DEGs

We used an online analysis tool created by David (https://david.ncifcrf.gov/) to perform gene ontology (GO) analysis and Kyoto Encyclopedia of Genes and Genomes (KEGG) analysis for all the 183 immune-related DEGs[11]. GO analysis classified the DEGs into three groups: molecular function group, biological process group, and cellular component group. The biological results revealed that DEGs were primarily enriched in inflammatory response, positive regulation of ERP1 and ERK2 cascade, and immune response (fig 1 C). The cellular component results indicated that DEGs were mainly enriched in extracellular space, an integral component of the plasma membrane (fig 1 D). The molecular function results showed that DEGs were mainly enriched in semaphorin receptor binding, chemokine activity, and cytokine activity (fig 1 E). Moreover, KEGG analysis indicated that the DEGs' pathways were mainly enriched in neuroactive ligand-receptor interaction and cytokine-cytokine receptor interaction (fig 1 F).

Training and test sets

We divided 289 samples into a training set (n=203) and a test set (n=86). The two sets satisfied the following criteria: 1. Samples were randomly divided into two sets; 2. Age, clinical stage, and follow-up time between the two sets were similar. The clinical information obtained from the two sets is shown in Table 1.

Identification of survival genes from the immune-related DEGs in the training set

Firstly, we used univariate Cox proportional hazard regression to analyze the RNAseq expression and survival date of all the 183 DEGs in the training set. Secondly, LASSO Cox regression analysis was used to analyze the valuable DEGs. Finally, multivariate Cox regression analysis was performed to identify survival DEGs. R package "survival" and "glmnt' were used for the above calculation, and $p<0.05$ was considered to be statistically significant. Univariate Cox regression analysis results identified 39 DEGs (Table 2), of which, five were left after conducting LASSO Cox regression analysis for a thousand times (fig 2 A-B). Finally, four DEGs (*NTS*, *BIRC5*, *ELN*, and *CHGA*) were selected as the survival genes after conducting multivariate Cox regression analysis (Table 3).

The survival state, risk score, and heatmap of 4 hub genes in the training set were showed (fig 2 C-E).

Analysis of hub DEGs

Three hub genes (*NTS*, *ELN*, and *CHGA*) had lower mRNA expression and one hub gene (*BIRC5*) had higher mRNA expression in primary cancer tissue compared to the normal kidney tissue (fig 3 A). In addition, Kaplan-Meier analysis results indicated that three genes (*BIRC5*, *ELN*, and *CHGA*) were survival-related (fig 3 B-E). We used the STRING online tool (https://string-db.org/)[12] to determine the protein-protein interactive relationship of the four hub genes (fig 3 F). The DNA methylation analysis function of ualcan (http://ualcan.path.uab.edu/)[13] revealed that DNA hyper-methylation occurred as a result of high-level mRNA expression of *BIRC5* (p=0.0013, fig 4 C).

The cbioportal website (https://www.cbioportal.org/)[14] was then used to explore the genetic alterations (fig 4 A) and copy numbers (CNV, fig 4 D) of the four hub genes. On the other hand, the ACB website (https://www.aclbi.com/static/index.html)[15] indicated that *ELN* gene expression was correlated with tumor mutation load (TMB, p=0.01, fig 4 B). We also investigated the variable shear situation of the four hub genes in the TSVdb website (http://www.tsvdb.com/)[16]. Results obtained from the online single-cell library of CancerSea (http://biocc.hrbmu.edu.cn/CancerSEA/, fig 4 E)[17] indicated that the mRNA expression of *ELN* was associated with angiogenesis (correlation=0.44, p <0.05, fig 4 F).

Prognostic value verification of the 4-mRNA signature in the training set and test set

The risk score of each patient was calculated based on the coefficients: Risk score = (0.250656*Exp NTS) + (0.465259*Exp BIRC5) + (0.251223*Exp ELN) + (0.241936*Exp CHGA). We found that the 4-mRNA signature risk score was an independent factor in multivariate Cox analysis (table 4).

A total of 203 samples in the training set were divided into high-risk score group (n=101) and low-risk score group (n=102) according to the risk score. A comparison of the two groups indicated that the high-risk score group had a higher mortality rate, while the low-risk score group had a large number of surviving patients (fig 3 C-E). Moreover, similar results were observed when 86 samples in the test set were divided into high-risk score group (n=42) and low-risk score group (n=44).

We also performed Kaplan-Meier analysis and ROC analysis for risk score on the training set and test set. Kaplan-Meier analysis in the training set found that the high-risk score group had a significantly shorter overall survival time (p =0.0041, fig 5 A), while and the ROC curves showed that the 4-mRNA signature had good accuracy with 0.957 in 1 year, 0.965 in 2 years, and 0.901 in 3 years (fig 5 A). 2. On the other hand, Kaplan-Meier analysis in the test set indicated that the high score group also had a significantly shorter overall survival time (p =0.021, fig 5 B), and the time-dependent ROC curves had good accuracy (0.963 in 1 year, 0.898 in 2 years, and 0.742 in 3 years, fig 5 B). Furthermore, nomogram models for the training set were drawn (fig 5 B).

Correlation between risk score and clinical feature

We analyzed the correlation between risk score and different clinical information (tumor, lymph node, metastasis degrees, and grades). The results showed that the risk score had significant differences in tumor, lymph node, metastasis degrees, and grades (fig 6 A). Moreover, time-dependent ROC analysis found that the 4-mRNA signature had better accuracy compared to other clinical features (fig 6 B).

The relationship between the risk score and immune cell component, expression of immune-related genes, and immunotherapy response

We explored the immune cell component using two online analysis tools (TIMER: https://cistrome.shinyapps.io/timer/[18] and ImmuCellAI: http://bioinfo.life.hust.edu.cn/ImmuCellAI/[19]). TIMER analysis results showed that a significantly higher percentage of B cells (P=0.0029), T cell+CD4 (P=0.0002), T cell+CD8 (P=0.0029), Neutrophil cells (P=0.0004), and DC cells (P=0.0047) would appear in the high-risk score group in the training set (fig 7 A). On the other hand, ImmuCellAI analysis results indicated that the high-risk score group had a higher percentage of Exhausted cells (P=0.00003) and B cells (P=0.0003) (fig 7 B). We also analyzed the expression of seven immune-related genes (*CTLA4*, *CD274*, *LAG3*, *SIGLEC15*, *PDCD1LG2*, *HAVCR2*, and *TIGIT*) and correlated the expression with the risk score. The results showed that *CTLA4*, *LAG3*, *PDCD1LG2*, and *TIGIT* had a higher expression in the high-risk score group (P<0.05, fig 7 C). In addition, the expression of *PDCD1LG2* and *TIGIT* genes correlated with the risk score value (P<0.05, fig 7 D-E). According to the immunotherapy response results obtained after ImmuCellAI analysis, the high-risk score group had a better immunotherapy response (P=0.0013, fig 7 F).

Discussion

In this study, we identified four hub mRNA genes (*NTS*, *BIRC5*, *ELN*, and *CHGA*) using univariate and multivariate Cox analysis, and LASSO analysis. Previous studies have reported that *NTS* is a neurotensin receptor that participates in the gastro-intestinal and cardiovascular functions[20,21]. Another study also found that the *NTS* gene activates the Wnt/β-catenin signaling pathway, thereby promoting tumor metastasis[22]. *BIRC5* is a member of the apoptosis inhibitor gene family, which encode regulatory proteins that prevent apoptotic cell death[23]. It regulates several types of cancer cells by activating a multiple-step cell apoptosis process[24,25]. *ELN* encodes the elastin protein, which is a key protein in the tumor microenvironment[26]. Moreover, the protein encoded by the *CHGA* gene is a member of the chromogranin/secretogranin family of neuroendocrine secretory proteins[27]. Its gene product is a precursor of the peptides which act as autocrine or paracrine negative modulators of the neuroendocrine system[28].

We then verified the prognostic value of the signature in both training and test sets. Kaplan-Meier analysis showed that the high-risk score group had a bad survival time, while ROC analysis found that the AUC of the signature was excellent (0.957 in 1 year, 0.965 in 2 years, and 0.901 in 3 years in the training set). A previous study had developed a 5-mRNA genes signature for pRCC patients and proved that the AUC of the signature was 0.82[29]. Furthermore, we conducted a correlation between the risk score and clinical classification, and found that the risk score was correlated with the TNM stage. The above results convinced us that the signature had an accurate prognostic value.

Finally, we conducted an analysis of the immune component and found different immune components in the two risk score groups. TIMER and ImmuCellAI analyses results indicated that the high-risk score group had a higher percentage of B cells in the immune component. Moreover, we conducted a correlation between the risk score and expression of immune-related genes. Our results indicated that the high-risk score group had a higher expression level of *CTLA4*, *LAG3*, *PDCD1LG2*, and *TIGIT*. In addition, the high-risk score group had a better immunotherapy response.

In summary, this study has identified four hub immune-related genes (*NTS*, *BIRC5*, *ELN*, and *CHGA*) in pRCC patients. We also developed a signature of four hub genes which can act as an independent prognostic factor for overall survival. Our results suggest that pRCC patients with a high-risk score have a shorter survival time and a better immunotherapy response.

Table 1：the clinical information of the training set and the test set

	The training set	The test set
Cases(n)	203	86
Age (>60 years old; <60 years old, n)	115, 88	55, 31
Sex (male, female, n)	154, 49	58, 28
T stage (T1, T2, T3, T4, Tx, n)	134, 26, 40, 2, 1	60, 6, 19, 0, 1
N stage (N0, N1, N2, Nx, n)	35, 17, 1, 150	15, 7, 3, 61
M stage (M0, M1, Mx, n)	72, 6, 125	30, 3, 53
Grade stage (I, II, III, IV, n)	122, 18, 53, 10	58, 3, 19, 6
Statue (alive, dead, n)	175, 28	70, 16

Table 2: TOP 10 genes in univariate Cox analysis

Gene id	HR	HR.95L	HR.95H	P value
BIRC5	2.155273	1.648415	2.817979	1.98E-08
CHGA	1.268253	1.150524	1.398028	1.75E-06
ELN	1.532013	1.256153	1.868453	2.54E-05
CCL19	1.297936	1.13736	1.481184	0.000109
LEFTY2	1.329668	1.127774	1.567704	0.000696
IL17B	1.631201	1.226547	2.169357	0.000769
NR3C2	0.494363	0.327281	0.746742	0.000815
NTS	1.325878	1.122007	1.566794	0.000928
VTN	1.240989	1.077436	1.42937	0.00275
CR2	1.266519	1.076726	1.489766	0.004339

Table 3 the hub 4 genes in multivariate Cox analysis

Gene id	coef	HR	HR.95L	HR.95H	P value
NTS	0.250656	1.284869	1.048373	1.574714	0.01573
BIRC5	0.465259	1.592426	1.189835	2.131239	0.001755
ELN	0.251223	1.285597	0.999556	1.653493	0.050406
CHGA	0.241936	1.273712	1.12858	1.437508	8.87E-05

Table 4 the clinical classier and risk score in multivariate Cox analysis

	coef	HR	HR.95L	HR.95H	P value
age	0.005597	1.005613	0.976774	1.035303	0.706164
gender	0.465879	1.593414	0.707722	3.587523	0.26055
grade	0.470943	1.601504	1.019282	2.516297	0.041072
T	0.10912	1.115296	0.757509	1.642073	0.580355
M	-0.00442	0.995594	0.723228	1.370533	0.9784
N	0.082667	1.08618	0.664299	1.775988	0.74176
Risk Score	0.048964	1.050183	1.028824	1.071985	3.00E-06

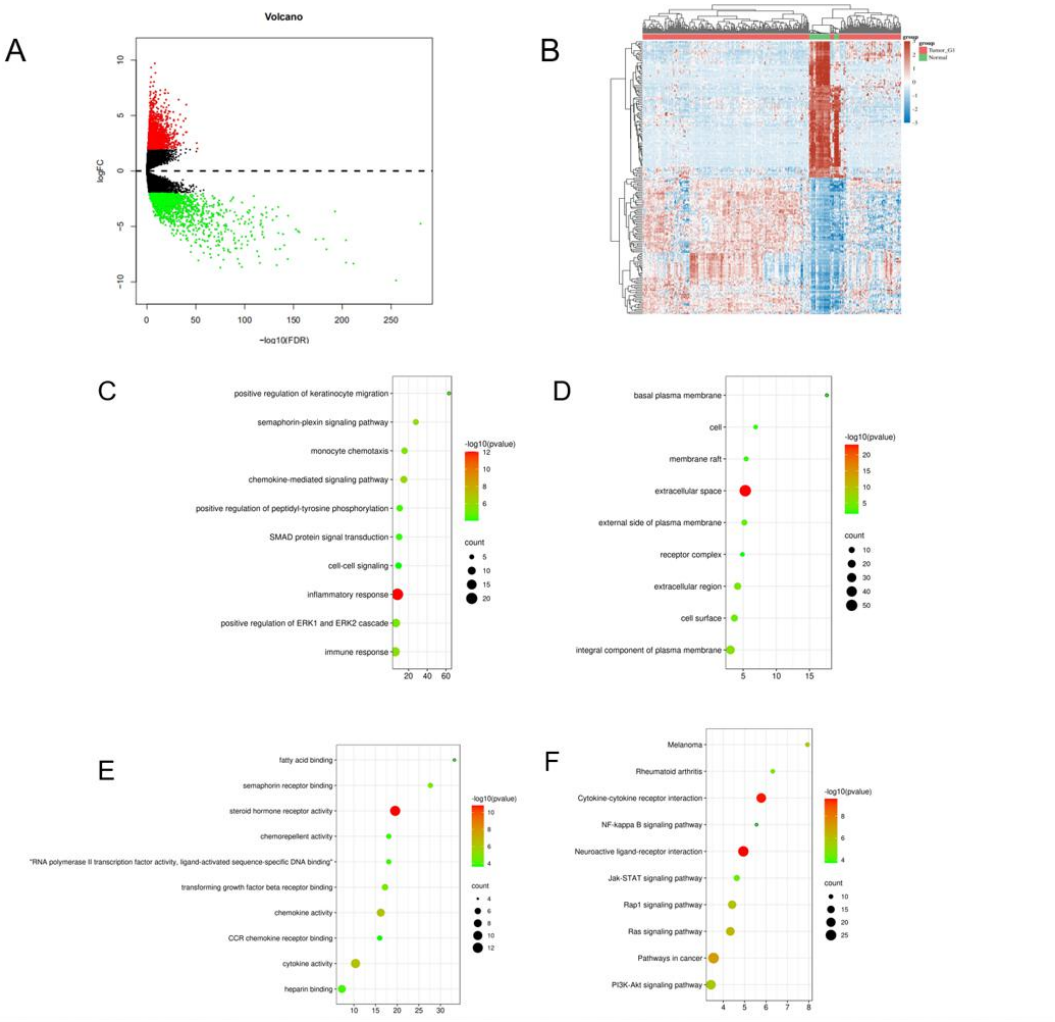

Fig 1. differential expression genes in TCGA KIRC data and enrichment analysis

A: Volcano plot in the differential expression genes (DEGs) in TCGA KIRC data; B: the heatmap of top 50 DEGs; C: the biological process in GO term; D: the cellular component in GO term; E: the molecular function in GO term; F: the pathway analysis in KEGG function.

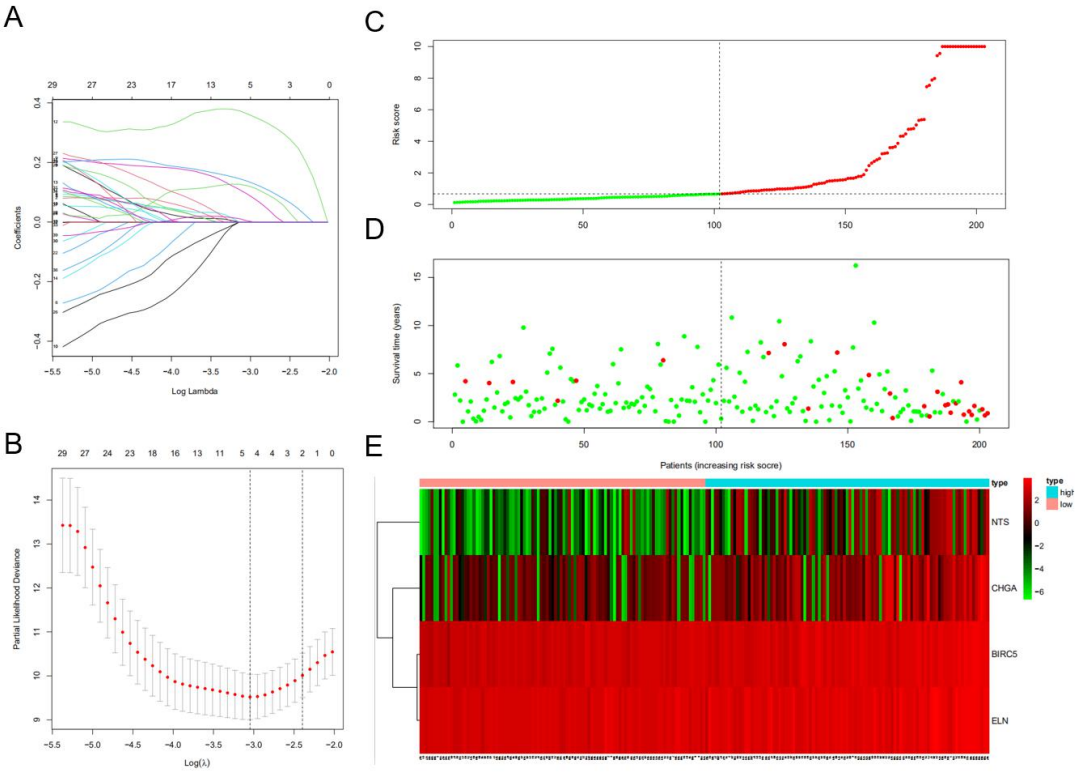

Fig 2 construction of the hub DEGs and risk score prognostic value

A, B: the determination of the number of factors by the LASSO analysis; C: the distribution of risk score patients; D: the survival state of patients; E: a heatmap of hub DEGs in the training set

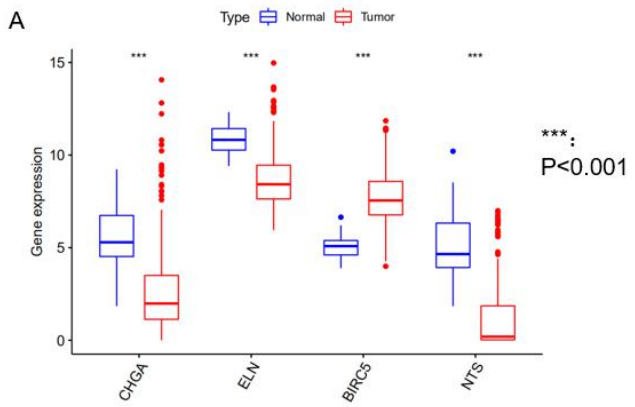

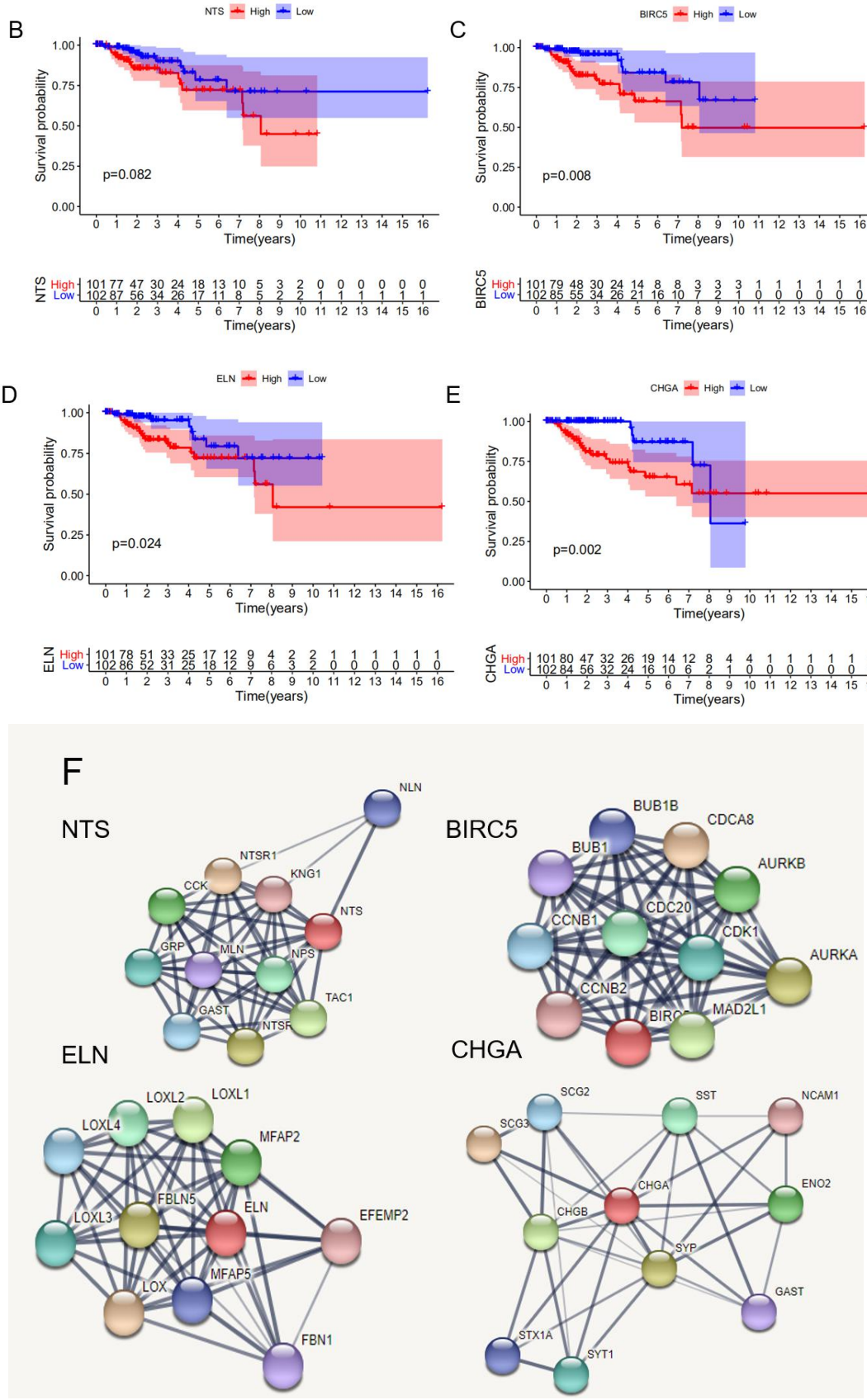

Fig 3 the analysis of hub DEGs' expression, survival results, and protein-protein interaction

A: the mRNA expression of 4 hub DEGs in normal vs tumor tissue; B-E: the survival results in Kaplan-Meier analysis; F: the protein-protein interaction of 4 hub DEGs.

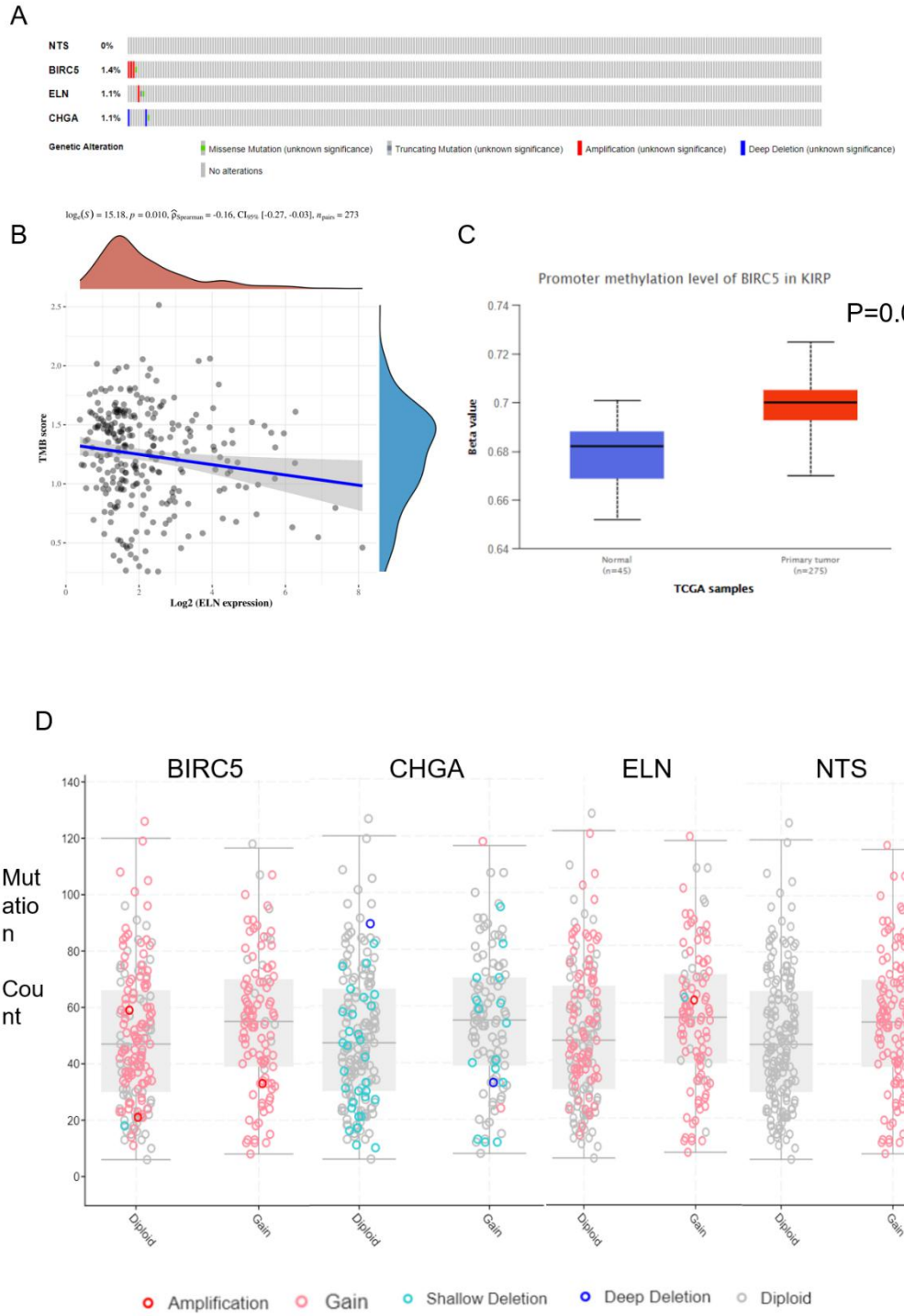

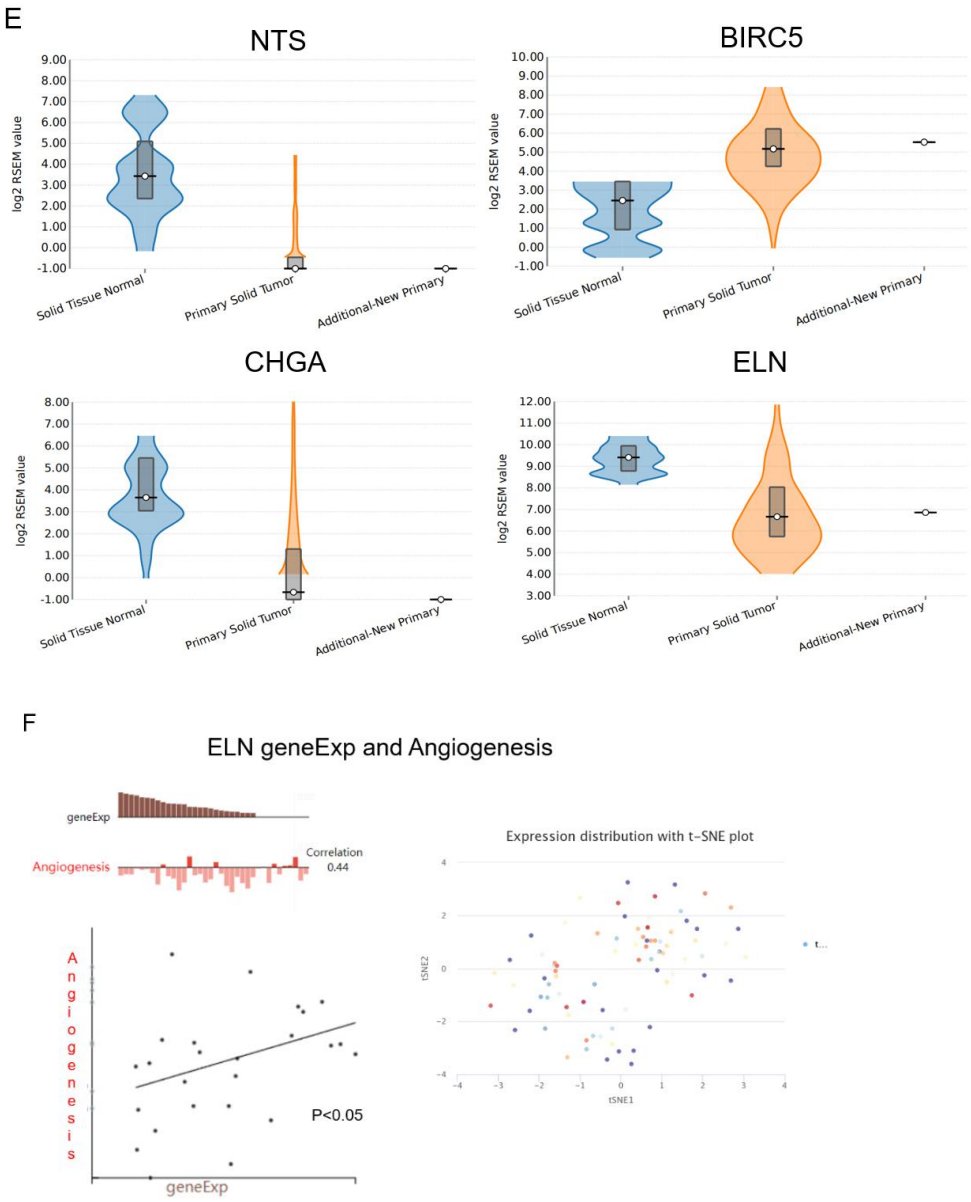

Fig 4 the analysis of hub DEGs' DNA methylation, TMB, CBV, and variable shear

A: the genetic alterations of four hub DEGs; B: the correlation between ELN geneEpx and TMB; C: the correlation between BIRC5 geneEpx and DNA methylation level; D: the correlation between hub DEGs geneEpx and CNV; E: the correlation between hub DEGs geneEpx and variable shear; F: the correlation between ELN geneEpx and Angiogenesis.

A： in the training set

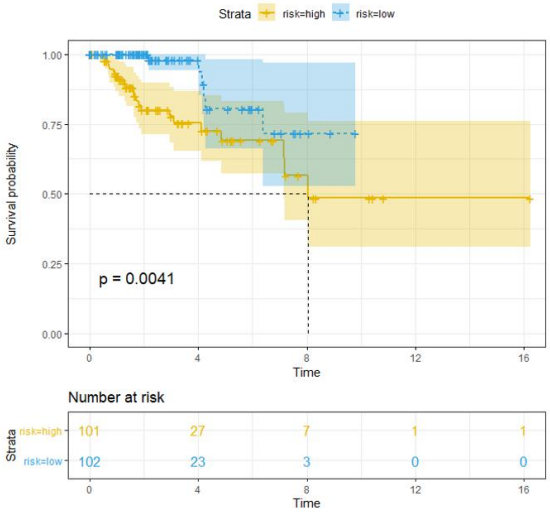

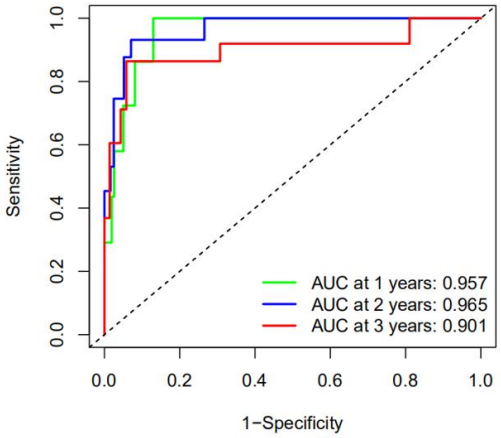

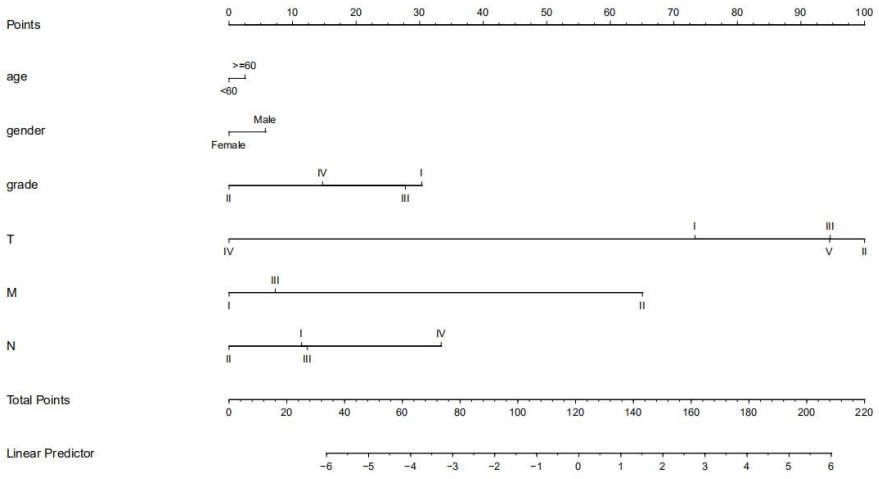

B： in the test set

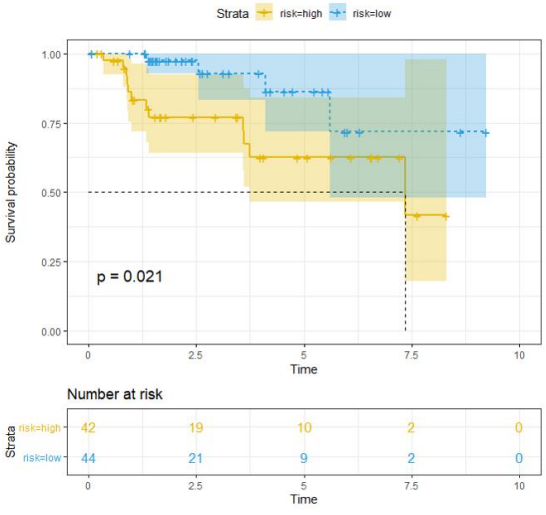

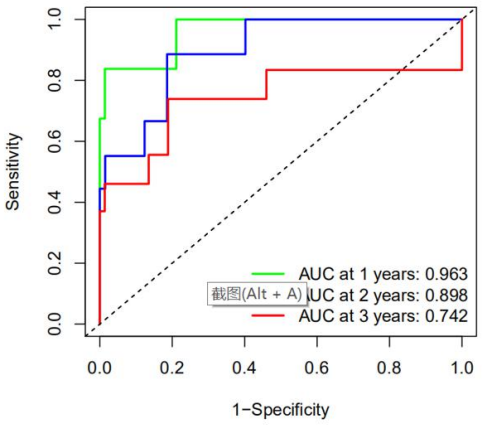

Fig 5 KM analysis and ROC analysis of risk score value in both sets

A: KM analysis, ROC analysis, and clinical nomogram model of risk score value in the training set;

B: KM analysis, and ROC analysis of risk score value in the test set.

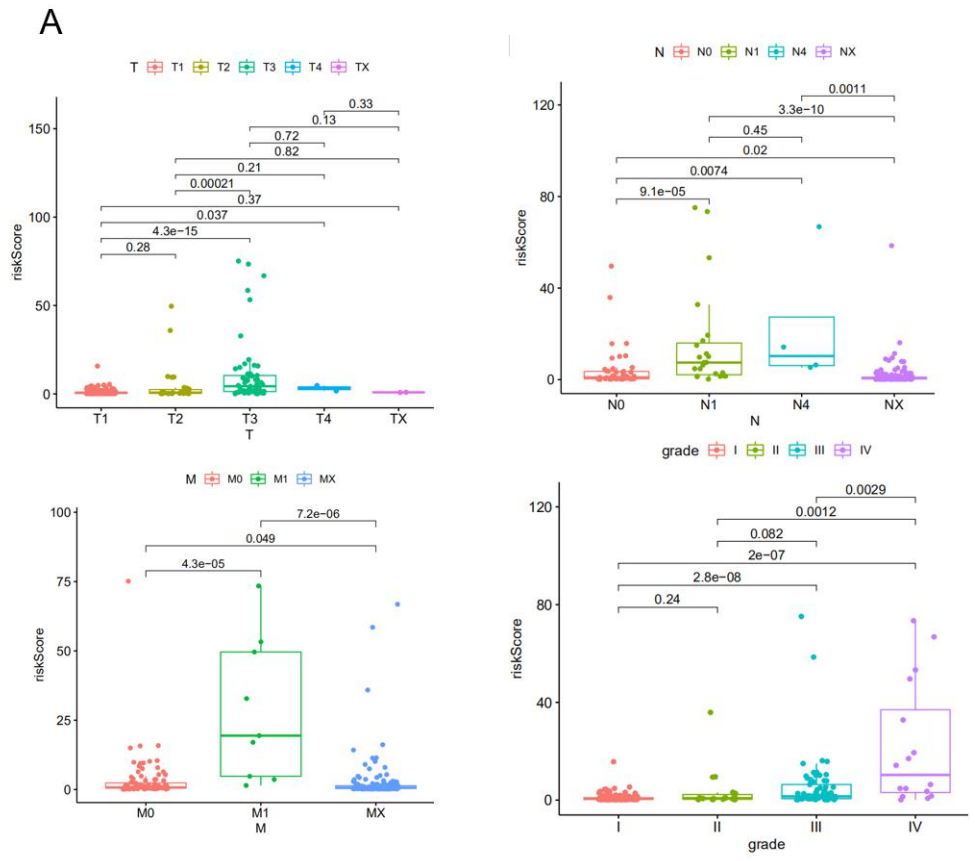

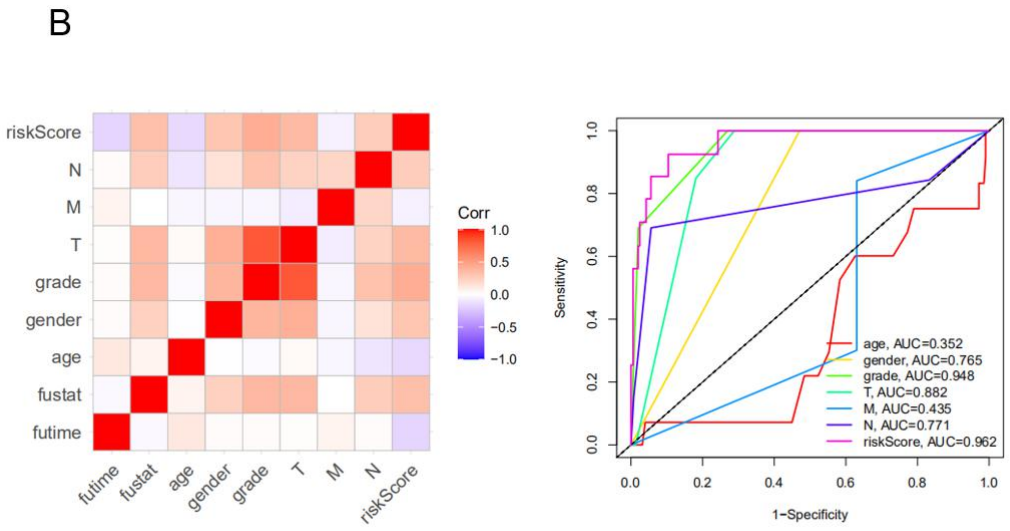

Fig 6 the correlation between the risk score and clinical classier

A: the correlation between the risk score and TNM grade information; B: the ROC.

A

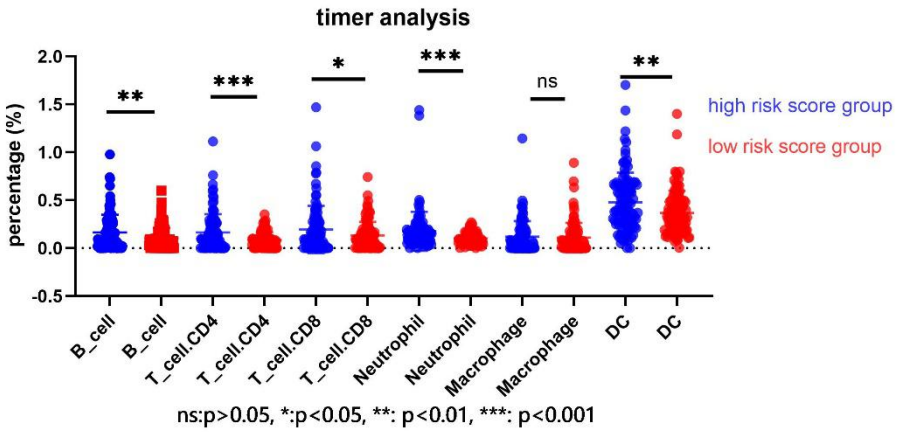
timer analysis
percentage (%)
high risk score group
low risk score group
B_cell
T_cell.CD4
T_cell.CD8
Neutrophil
Macrophage
DC
ns:p>0.05, *:p<0.05, **: p<0.01, ***: p<0.001

B

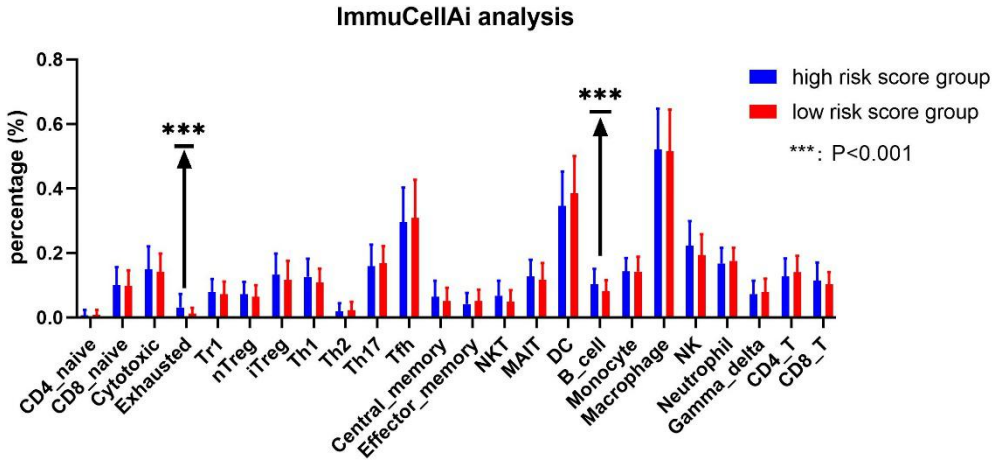
ImmuCellAi analysis
percentage (%)
high risk score group
low risk score group
***: P<0.001
CD4_naive
CD8_naive
Cytotoxic
Exhausted
Tr1
nTreg
iTreg
Th1
Th2
Th17
Tfh
Central_memory
Effector_memory
NKT
MAIT
DC
B_cell
Monocyte
Macrophage
NK
Neutrophil
Gamma_delta
CD4_T
CD8_T

C

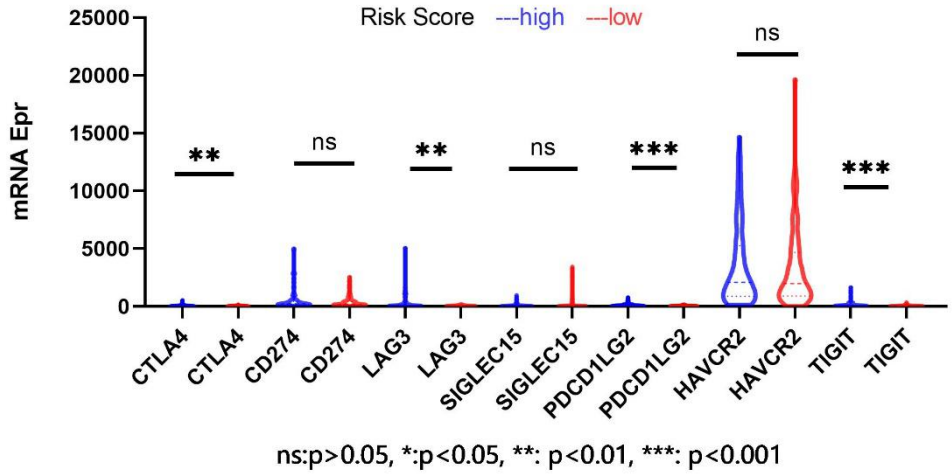
Risk Score ---high ---low
mRNA Epr
CTLA4
CD274
LAG3
SIGLEC15
PDCD1LG2
HAVCR2
TIGIT
ns:p>0.05, *:p<0.05, **: p<0.01, ***: p<0.001

D

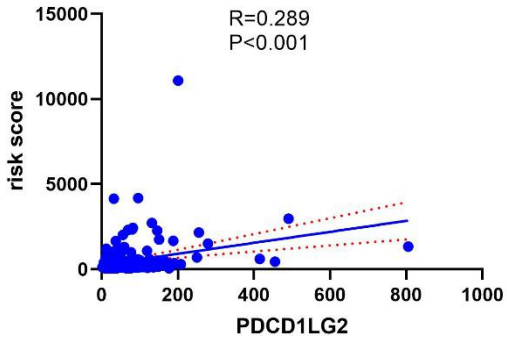

E

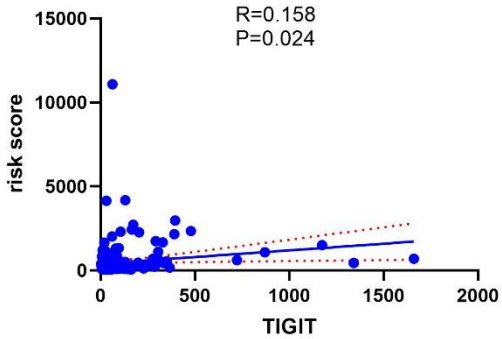

F

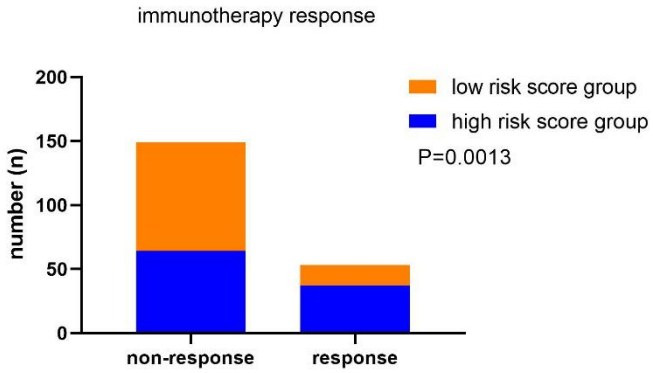

Fig 7 the relationship between the risk score and immune cell component, the immune-related genes' expression, and the immunotherapy response

A: the immune cell component in the web of timer; B: the immune cell component in the web of ImmuCellAI; C: the immune-related genes' expression in two groups; D-E: the correlation between the risk score and the immune-related genes; F: the immunotherapy response.

Declarations

Ethics approval and consent to participate

No application

Consent for publication

All the authors agreed to publish the paper.

Availability of data and material

We used the public data from TCGA KIRC data.

Author contributions

Shen junwen wrote the paper. Wang rongjiang and Zhang Lisha edited the paper. Chen yu, Fang zhihao, Yao jianxiang， Zhang xu and Ling yuhang analyzed the data. Tang jianer made the images out.

Funding

The Zhejiang province medical and health project (2020KY937)

disclosure

The authors have declared no conflicts of interest.

Reference:

1 Courthod, G., Tucci, M., Di Maio, M. & Scagliotti, G. V. Papillary renal cell carcinoma: A review of the current therapeutic landscape. *Critical reviews in oncology/hematology* **96**, 100-112, doi:10.1016/j.critrevonc.2015.05.008 (2015).

2 Kuroda, N. *et al.* Clear cell papillary renal cell carcinoma: a review. *International journal of clinical and experimental pathology* **7**, 7312-7318 (2014).

3 Chen, Q., Cheng, L. & Li, Q. The molecular characterization and therapeutic strategies of papillary renal cell carcinoma. *Expert review of anticancer therapy* **19**, 169-175, doi:10.1080/14737140.2019.1548939 (2019).

4 McDermott, D. F. *et al.* Clinical activity and molecular correlates of response to atezolizumab alone or in combination with bevacizumab versus sunitinib in renal cell carcinoma. *Nature medicine* **24**, 749-757, doi:10.1038/s41591-018-0053-3 (2018).

5 Rini, B. I. *et al.* The society for immunotherapy of cancer consensus statement on immunotherapy for the treatment of advanced renal cell carcinoma (RCC). *Journal for immunotherapy of cancer* **7**, 354, doi:10.1186/s40425-019-0813-8 (2019).

6 Rouprêt, M. *et al.* European Association of Urology Guidelines on Upper Urinary Tract Urothelial Carcinoma: 2020 Update. *European urology* **79**, 62-79, doi:10.1016/j.eururo.2020.05.042 (2021).

7 Huang, R., Mao, M., Lu, Y., Yu, Q. & Liao, L. A novel immune-related genes prognosis biomarker for melanoma: associated with tumor microenvironment. *Aging* **12**, 6966-6980, doi:10.18632/aging.103054 (2020).

8 Zhang, C. *et al.* Profiles of immune cell infiltration and immune-related genes in the tumor microenvironment of osteosarcoma. *Aging* **12**, 3486-3501, doi:10.18632/aging.102824 (2020).

9 Ritchie, M. E. *et al.* limma powers differential expression analyses for RNA-sequencing and microarray studies. *Nucleic acids research* **43**, e47, doi:10.1093/nar/gkv007 (2015).

10 Bhattacharya, S. *et al.* ImmPort: disseminating data to the public for the future of immunology. *Immunologic research* **58**, 234-239, doi:10.1007/s12026-014-8516-1 (2014).

11 Huang, D. W. *et al.* DAVID Bioinformatics Resources: expanded annotation database and

novel algorithms to better extract biology from large gene lists. *Nucleic acids research* **35**, W169-175, doi:10.1093/nar/gkm415 (2007).

12 Zhao, C. & Sahni, S. String correction using the Damerau-Levenshtein distance. *BMC bioinformatics* **20**, 277, doi:10.1186/s12859-019-2819-0 (2019).

13 Chandrashekar, D. S. *et al.* UALCAN: A Portal for Facilitating Tumor Subgroup Gene Expression and Survival Analyses. *Neoplasia (New York, N.Y.)* **19**, 649-658, doi:10.1016/j.neo.2017.05.002 (2017).

14 Unberath, P., Knell, C., Prokosch, H. U. & Christoph, J. Developing New Analysis Functions for a Translational Research Platform: Extending the cBioPortal for Cancer Genomics. *Studies in health technology and informatics* **258**, 46-50 (2019).

15 Bonneville, R. *et al.* Landscape of Microsatellite Instability Across 39 Cancer Types. *JCO precision oncology* **2017**, doi:10.1200/po.17.00073 (2017).

16 Sun, W. *et al.* TSVdb: a web-tool for TCGA splicing variants analysis.

17 Yuan, H. *et al.* CancerSEA: a cancer single-cell state atlas. *Nucleic acids research* **47**, D900-d908, doi:10.1093/nar/gky939 (2019).

18 Li, T. *et al.* TIMER: A Web Server for Comprehensive Analysis of Tumor-Infiltrating Immune Cells. *Cancer research* **77**, e108-e110, doi:10.1158/0008-5472.Can-17-0307 (2017).

19 Miao, Y. R. *et al.* ImmuCellAI: A Unique Method for Comprehensive T-Cell Subsets Abundance Prediction and its Application in Cancer Immunotherapy. *Advanced science (Weinheim, Baden-Wurttemberg, Germany)* **7**, 1902880, doi:10.1002/advs.201902880 (2020).

20 Qiu, S. *et al.* Exploratory Analysis of Plasma Neurotensin as a Novel Biomarker for Early Detection of Colorectal Polyp and Cancer. *Hormones & cancer* **10**, 128-135, doi:10.1007/s12672-019-00364-3 (2019).

21 Akter, H. *et al.* Activation of matrix metalloproteinase-9 (MMP-9) by neurotensin promotes cell invasion and migration through ERK pathway in gastric cancer. *Tumour biology : the journal of the International Society for Oncodevelopmental Biology and Medicine* **36**, 6053-6062, doi:10.1007/s13277-015-3282-9 (2015).

22 Ye, Y. *et al.* NTS/NTR1 co-expression enhances epithelial-to-mesenchymal transition and promotes tumor metastasis by activating the Wnt/β-catenin signaling pathway in hepatocellular carcinoma. *Oncotarget* **7**, 70303-70322, doi:10.18632/oncotarget.11854 (2016).

23 Gil-Kulik, P. *et al.* Increased Expression of BIRC2, BIRC3, and BIRC5 from the IAP Family in Mesenchymal Stem Cells of the Umbilical Cord Wharton's Jelly (WJSC) in Younger Women Giving Birth Naturally. *Oxidative medicine and cellular longevity* **2020**, 9084730, doi:10.1155/2020/9084730 (2020).

24 Sasso, E. *et al.* Replicative conditioning of Herpes simplex type 1 virus by Survivin promoter, combined to ERBB2 retargeting, improves tumour cell-restricted oncolysis. *Scientific reports* **10**, 4307, doi:10.1038/s41598-020-61275-w (2020).

25 Eslami, F. *et al.* Down-regulation of Survivin and Bcl-2 concomitant with the activation of caspase-3 as a mechanism of apoptotic death in KG1a and K562 cells upon exposure to a derivative from ciprofloxacin family. *Toxicology and applied pharmacology* **409**, 115331, doi:10.1016/j.taap.2020.115331 (2020).

26 Wang, Y., Song, E. C. & Resnick, M. B. Elastin in the Tumor Microenvironment. *Advances in experimental medicine and biology* **1272**, 1-16, doi:10.1007/978-3-030-48457-6_1 (2020).

27 Tutar, N. *et al.* Clinical significance of progastrin-releasing peptide, neuron-specific enolase, chromogranin a, and squamous cell cancer antigen in pulmonary neuroendocrine tumors. *Turkish journal of medical sciences* **49**, 774-781, doi:10.3906/sag-1810-147 (2019).

28 Eissa, N. *et al.* Chromogranin-A Regulates Macrophage Function and the Apoptotic Pathway in Murine DSS colitis. *Journal of molecular medicine (Berlin, Germany)* **96**, 183-198, doi:10.1007/s00109-017-1613-6 (2018).

29 Ahmad, A. *et al.* A five-gene signature predicts overall survival of patients with papillary renal cell carcinoma. *Plos One* **14**, doi:10.1371/journal.pone.0211491 (2019).

Figures

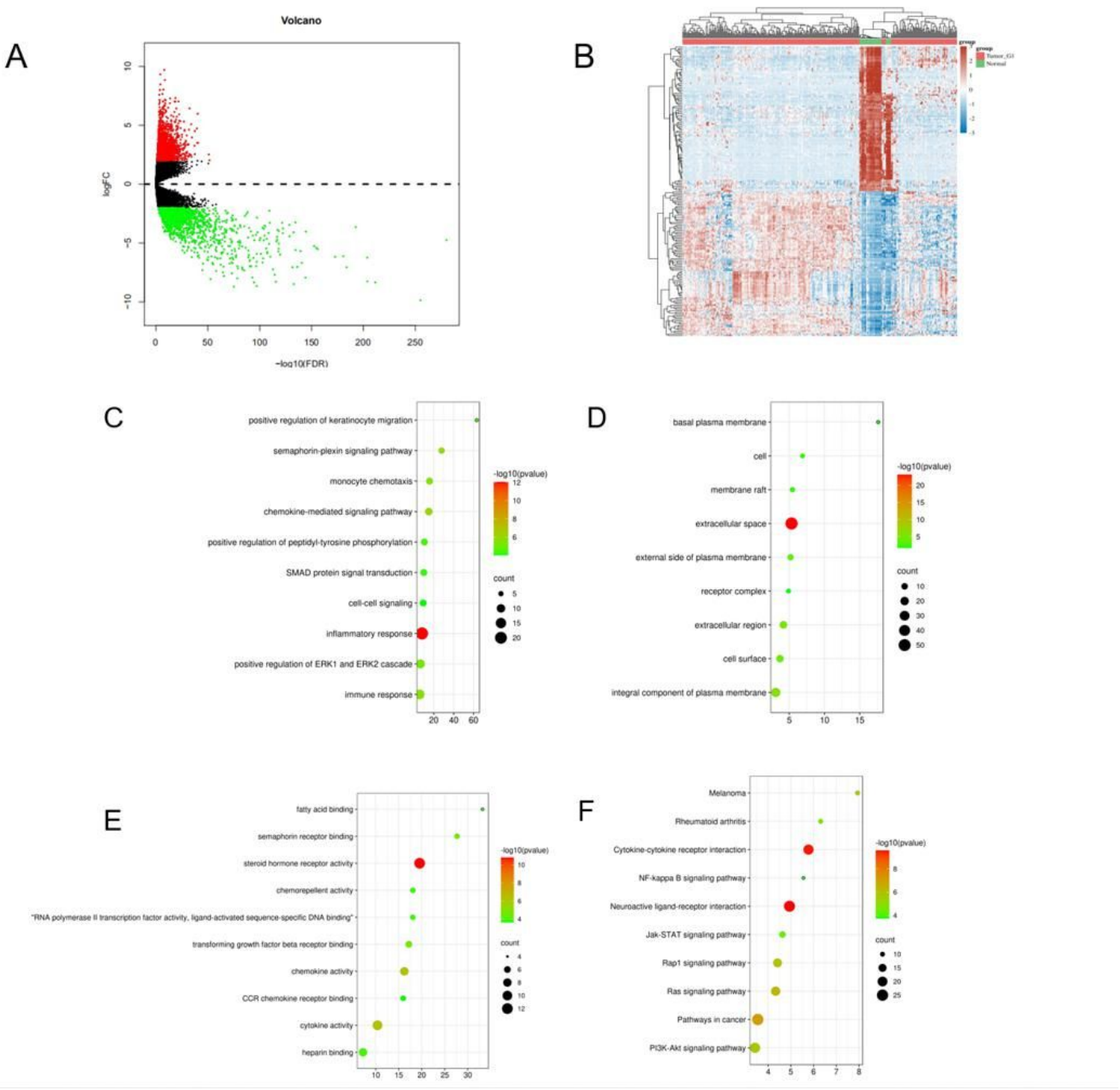

Figure 1

differential expression genes in TCGA KIRC data and enrichment analysis A: Volcano plot in the differential expression genes (DEGs) in TCGA KIRC data; B: the heatmap of top 50 DEGs; C: the biological process in GO term; D: the cellular component in GO term; E: the molecular function in GO term; F: the pathway analysis in KEGG function.

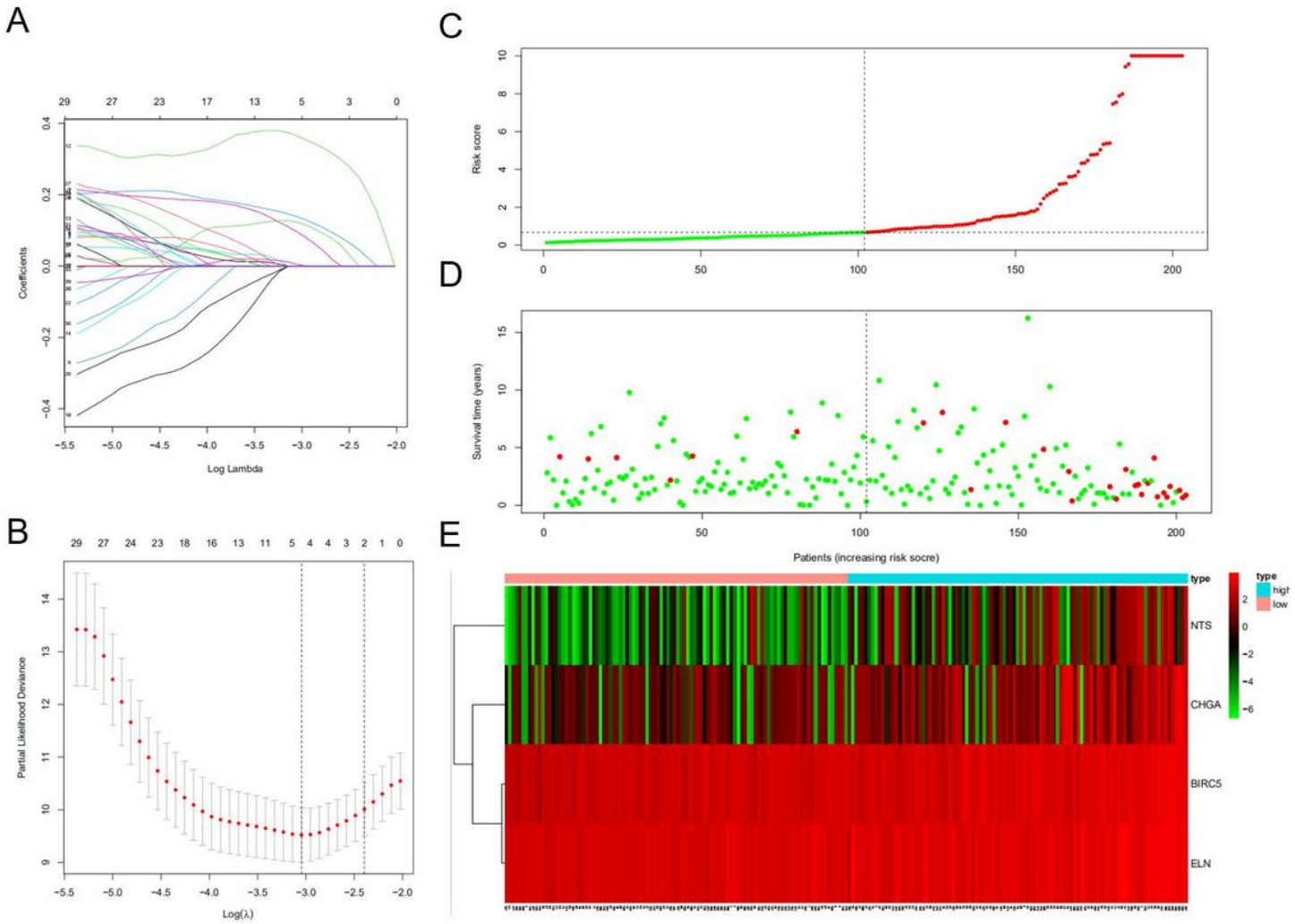

Figure 2

construction of the hub DEGs and risk score prognostic value A, B: the determination of the number of factors by the LASSO analysis; C: the distribution of risk score patients; D: the survival state of patients; E: a heatmap of hub DEGs in the training set

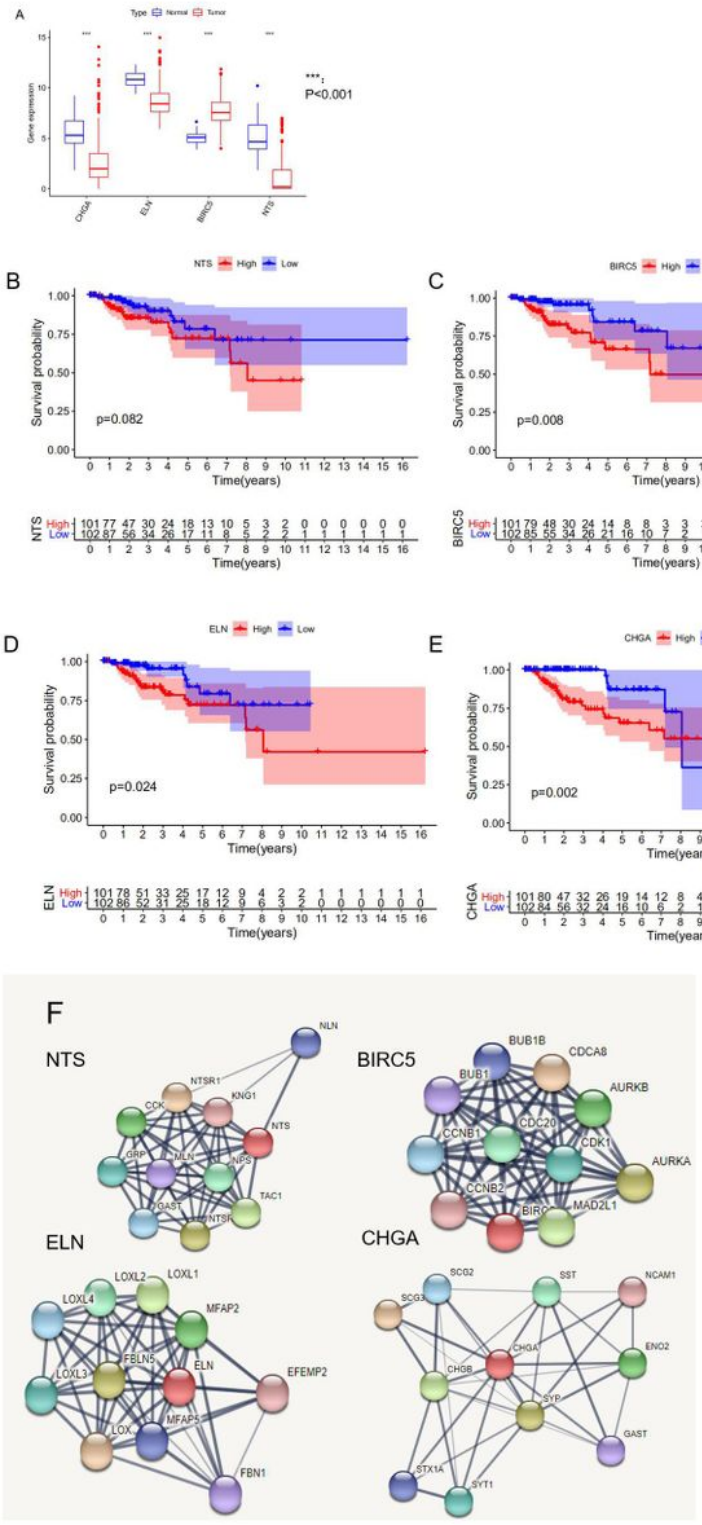

Figure 3

the analysis of hub DEGs' expression, survival results, and protein-protein interaction A: the mRNA expression of 4 hub DEGs in normal vs tumor tissue; B-E: the survival results in Kaplan-Meier analysis; F: the protein-protein interaction of 4 hub DEGs.

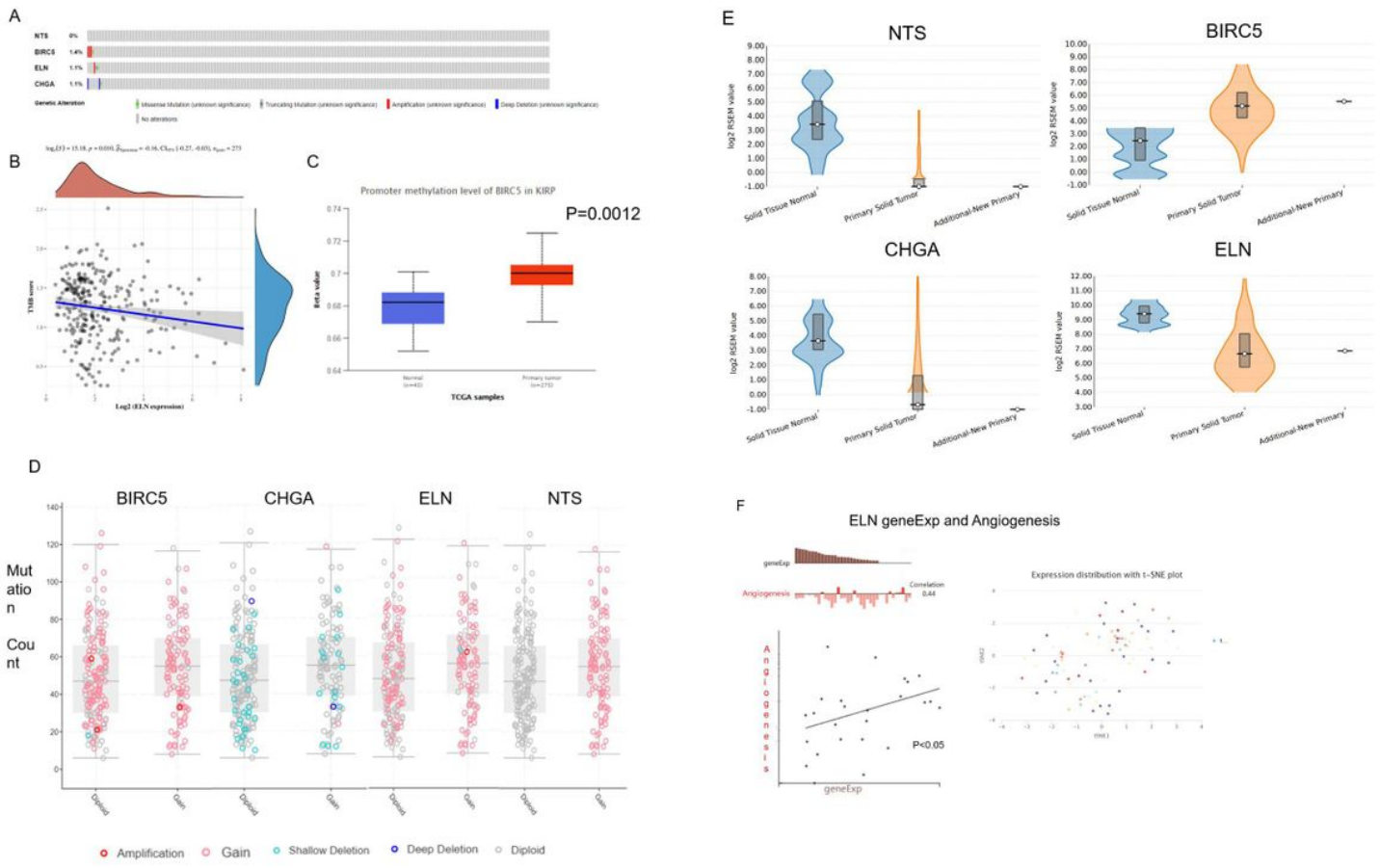

Figure 4

the analysis of hub DEGs' DNA methylation, TMB, CBV, and variable shear A: the genetic alterations of four hub DEGs; B: the correlation between ELN geneEpx and TMB; C: the correlation between BIRC5 geneEpx and DNA methylation level; D: the correlation between hub DEGs geneEpx and CNV; E: the correlation between hub DEGs geneEpx and variable shear; F: the correlation between ELN geneEpx and Angiogenesis.

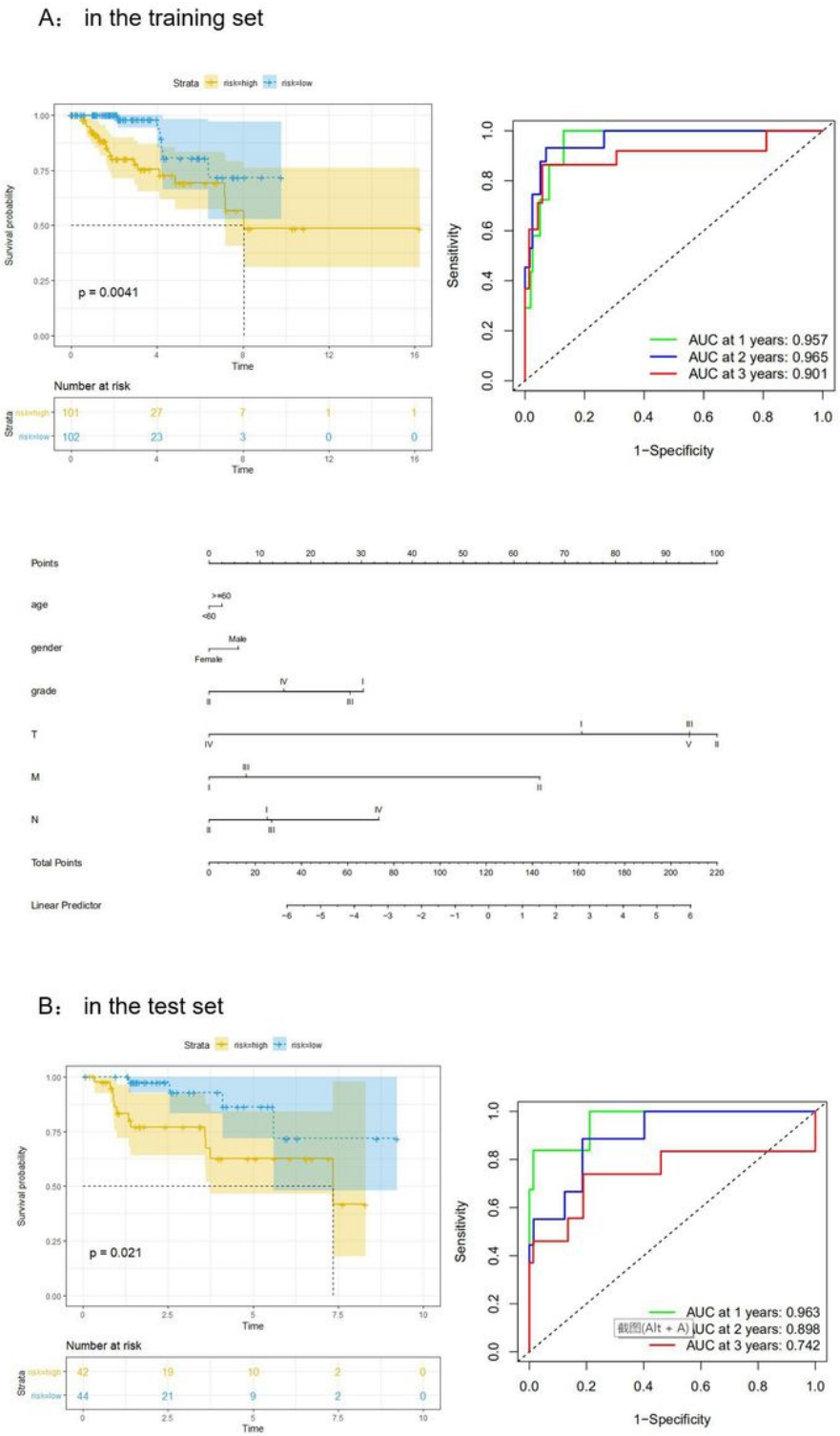

Figure 5

KM analysis and ROC analysis of risk score value in both sets A: KM analysis, ROC analysis, and clinical nomogram model of risk score value in the training set; B: KM analysis, and ROC analysis of risk score value in the test set.

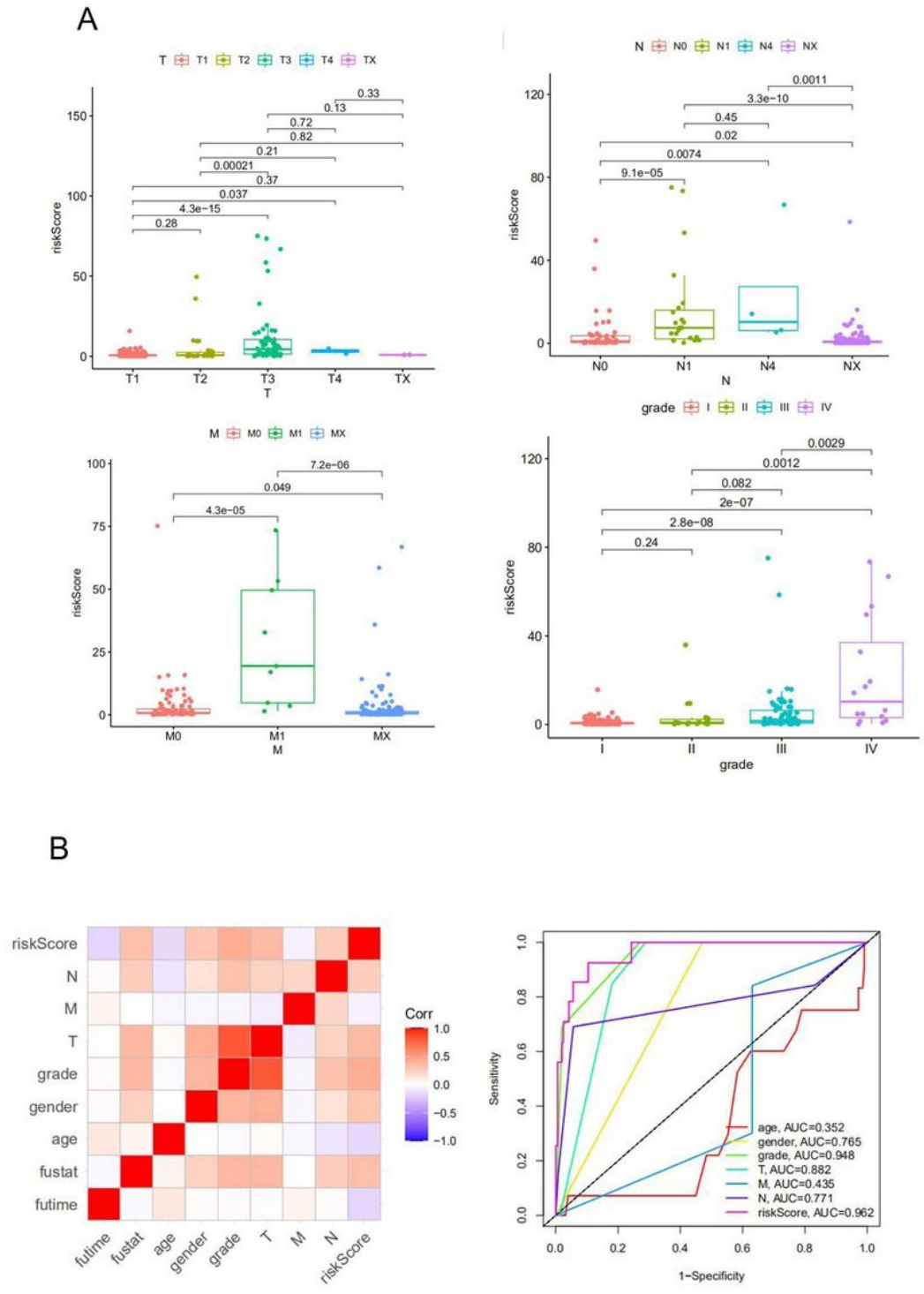

Figure 6

the correlation between the risk score and clinical classier A: the correlation between the risk score and TNM grade information; B: the ROC.

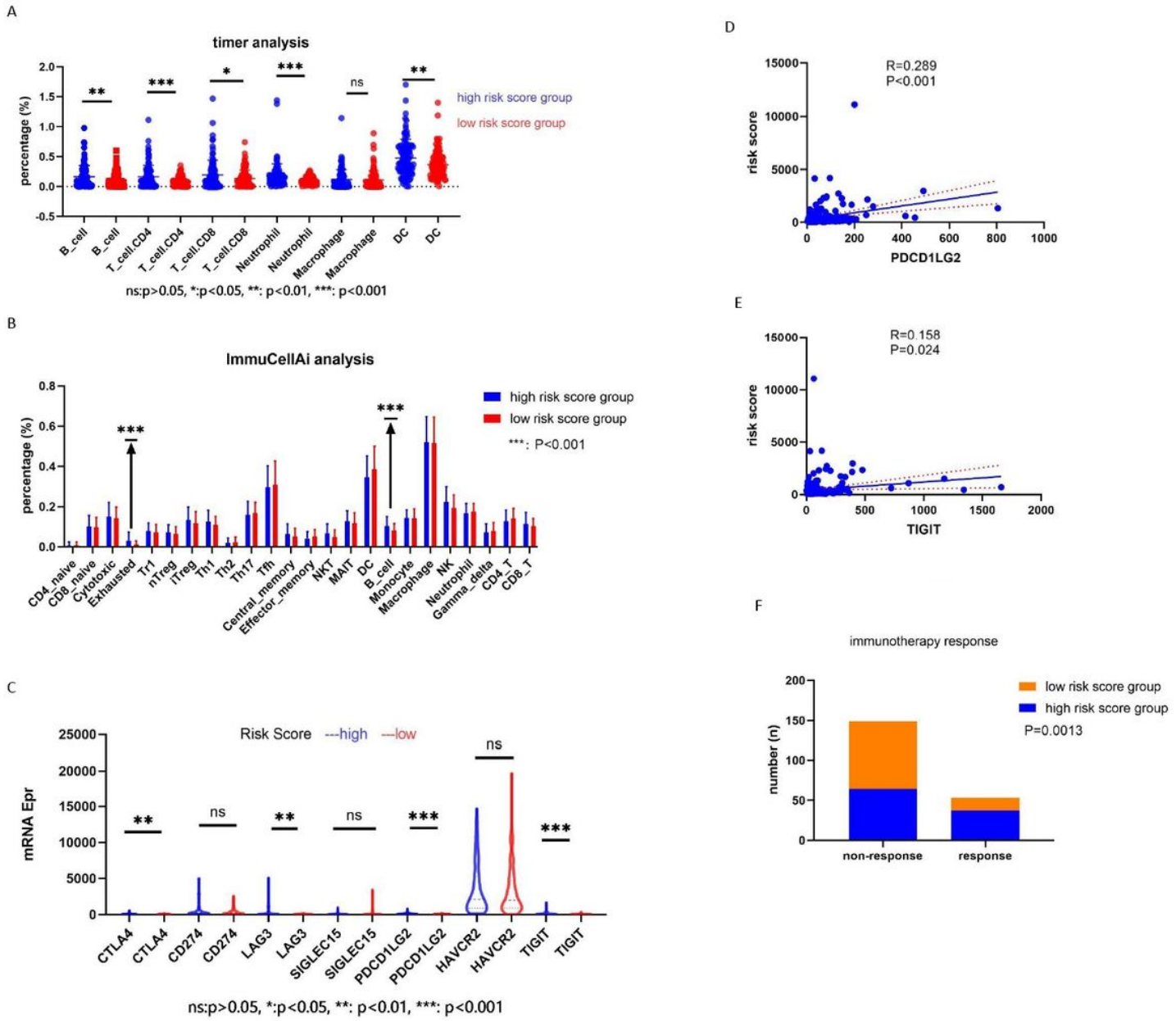

Figure 7

the relationship between the risk score and immune cell component, the immune-related genes' expression, and the immunotherapy response A: the immune cell component in the web of timer; B: the immune cell component in the web of ImmuCellAI; C: the immune-related genes' expression in two groups; D-E: the correlation between the risk score and the immune-related genes; F: the immunotherapy response.